

Branching ratios and CP asymmetries of the quasi-two-body decays $B_c \rightarrow K_0^*(1430, 1950)D_{(s)} \rightarrow K\pi D_{(s)}$ in the PQCD approach

Zhi-Qing Zhang¹, Zi-Yu Zhang¹, Ming-Xuan Xie¹, Ming-Yang Li¹, Hong-Xia Guo^{*2}

¹ *Institute of Theoretical Physics, School of Sciences, Henan University of Technology,
 Zhengzhou, Henan 450001, China*

² *School of Mathematics and Statistics, Zhengzhou University,
 Zhengzhou, Henan 450001, China*

October 10, 2024

Abstract

In this paper, we investigate the quasi-two-body decays $B_c \rightarrow K_0^*(1430, 1950)D_{(s)} \rightarrow K\pi D_{(s)}$ within the perturbative QCD (PQCD) framework. The S-wave two-meson distribution amplitudes (DAs) are introduced to describe the final state interactions of the $K\pi$ pair, which involve the time-like form factors and the Gegenbauer polynomials. In the calculations, we adopt two kinds of parameterization schemes to describe the time-like form factors: One is the relativistic Breit-Wigner (RBW) formula, which is usually more suitable for the narrow resonances, and the other is the LASS line shape proposed by the LASS Collaboration, which includes both the resonant and nonresonant components. We find that the branching ratios and the direct CP violations for the decays $B_c \rightarrow K_0^*(1430)D_{(s)}$ obtained from those of the quasi-two-body decays $B_c \rightarrow K_0^*(1430)D_{(s)} \rightarrow K\pi D_{(s)}$ under the narrow width approximation (NWA) can be consistent well with the previous PQCD results calculated in the two-body framework by assuming that $K_0^*(1430)$ is the lowest lying $\bar{q}s$ state, which is the so-called scenario II (SII). We conclude that the LASS parameterization is more suitable to describe the $K_0^*(1430)$ than the RBW formula, and the nonresonant components play an important role in the branching ratios of the decays $B_c \rightarrow K_0^*(1430)D_{(s)} \rightarrow K\pi D_{(s)}$. In view of the large difference between the decay width measurements for the $K_0^*(1950)$ given by BaBar and LASS collaborations, we calculate the branching ratios and the CP violations for the quasi-two-body decays $B_c \rightarrow K_0^*(1950)D_{(s)} \rightarrow K\pi D_{(s)}$ by using two values, $\Gamma_{K_0^*(1950)} = 0.100 \pm 0.04$ GeV and $\Gamma_{K_0^*(1950)} = 0.201 \pm 0.034$ GeV, besides the two kinds of parameterizations for the resonance $K_0^*(1950)$. We find that the branching ratios and the direct CP violations for the decays $B_c \rightarrow K_0^*(1950)D_{(s)} \rightarrow K\pi D_{(s)}$ have not as large difference between the two parameterizations as the case of decays involving the $K_0^*(1430)$, especially for the results with $\Gamma_{K_0^*(1950)} = 0.201 \pm 0.034$ GeV. The effect of the nonresonant component in the $K_0^*(1950)$ may be not so serious as that in the $K_0^*(1430)$. The quasi-two-body decays $B_c^+ \rightarrow K_0^{*+}(1430)D^0 \rightarrow K^0\pi^+D^0$ and $B_c^+ \rightarrow K_0^{*0}(1430)D^+ \rightarrow K^+\pi^-D^+$ have large branching ratios, which can reach to the order of 10^{-4} and are most likely to be observed in the future LHCb experiments. Furthermore, the branching ratios of the quasi-two-body decays $B_c \rightarrow K_0^*(1950)D_{(s)} \rightarrow K\pi D_{(s)}$ are about one order smaller than those of the corresponding decays $B_c \rightarrow K_0^*(1430)D_{(s)} \rightarrow K\pi D_{(s)}$.

I. INTRODUCTION

Recently, a lot of charmed three-body b-flavored heavy meson (B, B_s, B_c) decays have attract many attentions on the experimental side. For example, the decays $B^0 \rightarrow \bar{D}^{(*)0}K^+\pi^-$ [1,2], $B_s \rightarrow \bar{D}^{(*)0}K^-\pi^+$ [2,3], $B_s \rightarrow \bar{D}^0K^+K^-$ [4] and $B^0 \rightarrow D^+\pi^-\pi^-$ [5] have been measured in detail at LHCb. Many of these channels have large branching ratios, which are in the range $10^{-5} \sim 10^{-4}$. Besides being used to extract the unitary triangles in the standard model (SM), they provide a platform for probing the rich resonance structures and studying the localized CP violations. Many resonances have been found and studied in the such decays, for example, six $K\pi$ resonances were searched in the decay $B_s^0 \rightarrow \bar{D}^0K^-\pi^+$ [2]. It is helpful to understand the properties and inner structures of these resonances. As we know, the resonant contributions are commonly described by the relativistic Breit-Wigner (RBW) line shape, while such RBW parameterization is invalid for the broad-width resonances, such as $K_0^*(1430)$, which interferes

*Corresponding author: guohongxia@zzu.edu.cn

strongly with a slowly varying nonresonant background [6]. Then the so-called LASS lineshape [7] was suggested by the LASS collaboration to describe this resonance. In practice, different collaborations adopted different formulas to describe the $K_0^*(1430)$. For example, Belle employed the RBW model and an exponential parameterization to describe the resonant and nonresonant contributions in the $K_0^*(1430)$, respectively [8], while BaBar used the LASS parameterization to describe the $K_0^*(1430)$ resonance [9]. On the theoretical side, different parameterizations for the $K_0^*(1430)$ were also adopted by different authors. For example, the RBW formula was adopted to describe the $K_0^*(1430)$ in the decays $B \rightarrow K_0^*(1430)h \rightarrow K\pi h$ with h being π, K [10], while the LASS parameterization was used in the decays $B \rightarrow K_0^*(1430)D \rightarrow K\pi D$ [11]. Another scalar resonance $K_0^*(1950)$ with a little narrower width $\Gamma_{K_0^*(1950)} = 201 \pm 34$ MeV was observed in the LASS experiment for the reaction $K^-p \rightarrow K^-\pi^+n$ [7], where it was considered as a radial excitation of the 0^+ member with $L = 1$ triplet. Recently, its decay width was updated to $\Gamma_{K_0^*(1950)} = 80 \pm 38$ MeV by BaBar [12]. The underlying structures of the scalar mesons are long-standing puzzle and the classification of them is one of most interesting topics in hadron physics. Usually, there are two typical schemes for their classification: The nonet mesons below 1 GeV are viewed as the lowest lying $q\bar{q}$ states, while the nonet ones near 1.5 GeV including $K_0^*(1430)$ are suggested as the first excited states. It is called scenario I (SI). While in scenario II (SII), the nonet mesons near 1.5 GeV are treated as $q\bar{q}$ ground states, and the nonet mesons below 1 GeV are exotic states, such as four-quark bound states.

The B_c meson is the lowest-lying bound state of a bottom antiquark and a charm quark with $J^P = 0^-$. Because that both of its constituent quarks are heavy and can decay individually, a very rich B_c -decay channels with sizable branching ratios are expected, which will provide a unique platform for studying the weak decay mechanism of heavy flavor mesons. Since more than 10^{10} B_c events per year can be collected at LHC with the luminosity of $\mathcal{L} = 10^{34}$ cm $^{-2}$ s $^{-1}$ [13] at present, we will enter the precision era in B_c physics in the near future. Measurements of some B_c meson three-body decays, such as $B_c \rightarrow K^+K^-\pi^+$ [14], $B_c \rightarrow J/\Psi D^{(*)0}K^+$, $J/\Psi D^{(*)+}K^{*0}$ [15] have been performed. Furthermore, the two-body decays $B_c \rightarrow K_0^*(1430)D_{(s)}$ have been studied in previous work [16], where the branching ratios are predicted as $10^{-5} \sim 10^{-4}$. So large branching ratios can be detected by the future LHCb experiments. In view of upper listed reasons, we would like to study the scalar resonances $K_0^*(1430)$ and $K_0^*(1950)$ through the quasi-two-body decays $B_c \rightarrow K_0^*(1430, 1950)D_{(s)} \rightarrow K\pi D_{(s)}$ within the PQCD framework. In order to study $B_{(c)}$ meson three-body decays, many approaches based on symmetry principles and factorization theorems have been proposed. Symmetry principles include the U-spin [17–19], isospin and flavor $SU(3)$ symmetry [20–23], and the factorization-assisted topological-diagram amplitude (FAT) approach [24], etc. Factorization theorems include the QCD-improved factorization approach [25–29] and the PQCD approach [30–34]. It has been proposed that the factorization theorem of the quasi-two-body $B_{(c)}$ decays is approximately valid when the two particles move collinearly and the bachelor particle recoils back in the final states. This case corresponds to the edges of the Dalitz plot, which provides us a great opportunity to probe the properties of various resonances. According to this quasi-two-body-decay mechanism, the two-meson distribution amplitudes (DAs) are introduced into the PQCD approach, where the strong dynamics between the two final hadrons in the resonant regions are included.

This paper is organized as follows. The framework of the PQCD approach for the quasi-two-body B_c decays is reviewed in Section II, where the kinematic variables for each meson are defined and the S-wave $K\pi$ pair distribution amplitudes up to twist-3 are parametrized. Then, the analytical formulas of each Feynman diagram and the total amplitudes for these decays are listed. In Section III, the numerical results and discussions are presented. The final section is devoted to our conclusions. Some details related functions are collected in the Appendix.

II. THE FRAMEWORK

In the framework of the PQCD approach for the quasi-two-body decays, the factorization formulas for the $B_c \rightarrow K_0^*(1430, 1950)D_{(s)} \rightarrow K\pi D_{(s)}$ decay amplitudes can be written as [35, 36]

$$\mathcal{A} = \Phi_{B_c} \otimes H \otimes \Phi_{K\pi}^{\text{S-wave}} \otimes \Phi_{D_{(s)}}, \quad (1)$$

where $\Phi_{B_c}(\Phi_{D_{(s)}})$ denotes the DAs of the initial (final bachelor) meson, $\Phi_{K\pi}^{\text{S-wave}}$ is the S-wave $K\pi$ pair DAs, and \otimes denotes the convolution integrations over the parton momenta. Similar to the two-body decay case, the evolution of the hard kernel H for the b quark decay is calculable perturbatively and starts with the diagrams of single hard gluon exchange. The nonperturbative dynamics are absorbed into those DAs Φ_{B_c} , $\Phi_{D_{(s)}}$ and $\Phi_{K\pi}^{\text{S-wave}}$.

In the rest frame of the B_c meson, we define the B_c meson momentum p_{B_c} , the $K(\pi)$ meson momentum $p_1(p_2)$, the scalar meson K_0^{*1} momentum $p = p_1 + p_2$, and the bachelor meson $D_{(s)}$ momentum p_3 in light-cone coordinates as

$$p_{B_c} = \frac{m_{B_c}}{\sqrt{2}}(1, 1, \mathbf{0}_T), \quad p = \frac{m_{B_c}}{\sqrt{2}}(\zeta, 1 - r^2, \mathbf{0}_T), \quad p_3 = \frac{m_{B_c}}{\sqrt{2}}(1 - \zeta, r^2, \mathbf{0}_T), \quad (2)$$

¹From now on we use K_0^* to represent $K_0^*(1430)$ or $K_0^*(1950)$ for simplicity.

where the mass ratio $r = m_{D_{(s)}}/m_{B_c}$ and $\zeta = s/m_{B_c}^2$ with the invariant mass square $s = p^2 = m_{K\pi}^2$ for the $K\pi$ pair. The momenta of the light quarks in the initial meson B_c , the scalar meson K_0^* and the bachelor meson $D_{(s)}$ are defined as k_1, k and k_3 , respectively

$$k_1 = \frac{m_{B_c}}{\sqrt{2}}(x_1, 0, \mathbf{k}_{1T}), \quad k = \frac{m_{B_c}}{\sqrt{2}}(0, (1-r^2)z, \mathbf{k}_T), \quad k_3 = \frac{m_{B_c}}{\sqrt{2}}((1-\zeta)x_3, 0, \mathbf{k}_{3T}), \quad (3)$$

where x_1, z and x_3 are the corresponding momentum fractions.

A. WAVE FUNCTIONS

In the course of the PQCD calculations, the necessary inputs contain the DAs, which are constructed via the nonlocal matrix elements. Since the B_c meson is composed of two heavy quarks, one can take the nonrelativistic approximation form, that is the zero-point wave function, for the B_c meson light-cone distribution amplitudes (LCDAs)

$$\Phi_{B_c}(x) = \frac{if_{B_c}}{4N_c} [(\not{P} + m_{B_c}) \gamma_5 \delta(x - r_c)] \exp\left(-\frac{\omega_b^2 b^2}{2}\right), \quad (4)$$

where $N_c = 3$ is the color factor, the mass ratio $r_c = m_c/m_{B_c}$ and the shape parameter $\omega_b = 0.6 \pm 0.05$ GeV. Here, only the Lorentz structure offering the dominant contribution is considered, while the contribution from the other one is numerically small and can be neglected. The exponent term describes the intrinsic k_T -dependence with b being the conjugate space coordinate.

For D meson, the two-parton LCDAs in the heavy quark limit can be written as [37, 38]

$$\langle D(p) | q_\alpha(z) \bar{c}_\beta(0) | 0 \rangle = \frac{i}{\sqrt{2N_c}} \int_0^1 dx e^{ixp \cdot z} [\gamma_5 (\not{p} + m_D) \phi_D(x, b)]_{\alpha\beta}, \quad (5)$$

with the distribution amplitude $\phi_D(x, b)$,

$$\phi_D(x, b) = \frac{1}{2\sqrt{2N_c}} f_D 6x(1-x) [1 + C_D(1-2x)] \exp\left[\frac{-\omega^2 b^2}{2}\right], \quad (6)$$

where x is the momentum fraction of the light quark in D meson, $C_D = 0.5 \pm 0.1$, $\omega = 0.1$ GeV and $f_D = 211.9$ MeV. It is similar for the LCDAs of D_s meson but with different parameters $C_{D_s} = 0.4 \pm 0.1$, $\omega = 0.2$ GeV and $f_{D_s} = 249$ MeV, caused by a little SU(3) breaking effect [34].

The S -wave $K\pi$ system LCDAs are written as

$$\Phi_{K\pi}(z, s) = \frac{1}{\sqrt{2N_c}} [\not{v} \phi_0(z, s) + \sqrt{s} \phi_s(z, s) + \sqrt{s} (\not{v} \not{n} - 1) \phi_t(z, s)], \quad (7)$$

where the dimensionless vectors $v = (0, 1, 0_T)$ and $n = (1, 0, 0_T)$. The twist-2 LCDA is defined as

$$\phi_0(z, s) = \frac{F_{K\pi}(s)}{2\sqrt{2N_c}} \left\{ 6z(1-z) \left[a_0(\mu) + \sum_{m=1}^{\infty} a_m(\mu) C_m^{3/2}(2z-1) \right] \right\}, \quad (8)$$

where $C_m^{3/2}$ are the Gegenbauer polynomials, $a_0 = (m_s(\mu) - m_q(\mu)) / \sqrt{s}$ for K_0^{*-} , \bar{K}_0^{*0} and $a_0 = (m_q(\mu) - m_s(\mu)) / \sqrt{s}$ for K_0^{*+} , K_0^{*0} [39]. The scale-dependent Gegenbauer moments $a_1 = -0.57 \pm 0.13$ and $a_3 = -0.42 \pm 0.22$ at the scale $\mu = 1$ GeV for the resonance $K_0^*(1430)$, and the contributions from the even terms have been neglected [40]. Since the Gegenbauer moments for the resonance $K_0^*(1950)$ are not available at present, we will use the same Gegenbauer moments a_1 and a_3 with those for $K_0^*(1430)$ in the numerical calculations. As for the twist-3 LCDAs, we adopt the asymptotic forms as follows

$$\phi_s(z, s) = \frac{F_{K\pi}(s)}{2\sqrt{2N_c}}, \quad \phi_t(z, s) = \frac{F_{K\pi}(s)}{2\sqrt{2N_c}}(1-2z). \quad (9)$$

Here the time-like form factor $F_{K\pi}(s)$ is related to scalar form factor $F_0^{K\pi}(s)$ by the formula

$$F_{K\pi}(s) = \frac{m_K^2 - m_\pi^2}{m_{K_0^*}(m_s - m_q)} F_0^{K\pi}(s), \quad (10)$$

where q represents the light quark u or d , the scalar form factor $F_0^{K\pi}(s)$ is defined as [41–43]

$$\langle K\pi | \bar{q}s | 0 \rangle = C_X \frac{m_K^2 - m_\pi^2}{(m_s - m_q)} F_0^{K\pi}(s), \quad (11)$$

with the isospin factor $C_X = 1(1/\sqrt{2})$ for the $K^+\pi^-, K^0\pi^+(K^+\pi^0, K^0\pi^0)$ pairs. For the case of the $K^+\pi^-$ pair originated from the resonant state $K_0^{*0}(1430)$, we can insert a complete of $K_0^{*0}(1430)$ intermediate state into above matrix elements [42]

$$\langle K^+\pi^- | \bar{d}s | 0 \rangle_{K_0^*} \approx \langle K^+\pi^- | K_0^{*0} \rangle \frac{1}{\mathcal{D}_{K_0^*}} \langle K_0^{*0} | \bar{d}s | 0 \rangle = \frac{g_{K_0^* K \pi}}{m_{K_0^*}^2 - s - im_{K_0^*} \Gamma(s)} m_{K_0^*} \bar{f}_{K_0^*}, \quad (12)$$

where the definitions of the scalar decay constant $\bar{f}_{K_0^*}$ and the coupling constant $g_{K_0^* K \pi}$, i.e., $\langle K_0^{*0} | \bar{d}s | 0 \rangle = m_{K_0^*} \bar{f}_{K_0^*}$ and $g_{K_0^* K \pi} = \langle K^+\pi^- | K_0^{*0} \rangle$, have been used. The scale-dependent scalar decay constant $\bar{f}_{K_0^*}$ is related with the vector decay constant $f_{K_0^*}$ by the equations of motion $\bar{f}_{K_0^*} = \frac{m_{K_0^*} f_{K_0^*}}{m_s(\mu) - m_d(\mu)}$. We will employ $f_{K_0^*(1430)} m_{K_0^*(1430)}^2 = 0.0842 \pm 0.0045 \text{GeV}^3$ [44] and $f_{K_0^*(1950)} m_{K_0^*(1950)}^2 = 0.0414 \text{GeV}^3$ [45] in the following calculations. The mass-dependent decay width $\Gamma(s)$ in the denominator is related with the total decay width Γ_0 of K_0^* by the formula $\Gamma(s) = \Gamma_0 \frac{q}{q_0} \frac{m_{K_0^*}}{\sqrt{s}}$ with q being the magnitude of the momentum for the daughter meson K or π

$$q = \frac{1}{2} \sqrt{[s - (m_K + m_\pi)^2][s - (m_K - m_\pi)^2]} / s. \quad (13)$$

The q_0 in $\Gamma(s)$ is the value for q at $s = m_{K_0^*}^2$. The coupling constant $g_{K_0^* K \pi}$ is determined from the partial width $\Gamma_{K_0^* \rightarrow K \pi}$ for the decay $K_0^* \rightarrow K \pi$ through the relation [46]

$$g_{K_0^* K \pi} = \sqrt{\frac{8\pi m_{K_0^*}^2 \Gamma_{K_0^* \rightarrow K \pi}}{q_0}}. \quad (14)$$

It is noticed that the LASS parametrization is often used to describe the S -wave $K\pi$ system, especially for $K_0^*(1430)$ in experiments [47],

$$R(s) = \frac{\sqrt{s}}{q \cot \delta_B - iq} + e^{2i\delta_B} \frac{m_{K_0^*} \Gamma_0 \frac{m_{K_0^*}}{q_0}}{m_{K_0^*}^2 - s - im_{K_0^*} \Gamma_0 \frac{q}{\sqrt{s}} \frac{m_{K_0^*}}{q_0}}, \quad (15)$$

where $\cot \delta_B = \frac{1}{aq} + \frac{1}{2}rq$ with the scattering length $a = 2.07 \pm 0.10 \text{GeV}^{-1}$ and the effective range $r = 3.32 \pm 0.34 \text{GeV}^{-1}$ [47]. The first (second) term refers to the nonresonant (resonant) contribution. If using the LASS parametrization to replace the RBW formula in the scalar form factor $F^{K\pi}(s)$, one can get the time-like form factor $F_{K\pi}(s)$

$$F_{K\pi}(s) = \frac{q_0}{m_{K_0^*}^2 \Gamma_0} g_{K_0^* K \pi} \bar{f}_{K_0^*} R(s). \quad (16)$$

For comparison, these two parametrizations are used in the numerical calculations.

B. Analytic formulae

For the quasi-two-body decays $B_c \rightarrow K_0^* D_{(s)} \rightarrow K\pi D_{(s)}$, the effective Hamiltonian relevant to the $b \rightarrow s(d)$ transition is given by [48]

$$H_{eff} = \frac{G_F}{\sqrt{2}} \left\{ \sum_{q=u,c} V_{qb} V_{qs(d)}^* \left[C_1(\mu) O_1^{(q)}(\mu) + C_2(\mu) O_2^{(q)}(\mu) \right] - \sum_{i=3 \sim 10} V_{tb} V_{ts(d)}^* C_i(\mu) O_i(\mu) \right\} + H.c., \quad (17)$$

where the Fermi coupling constant $G_F \simeq 1.166 \times 10^{-5} \text{GeV}^{-2}$, $V_{qb} V_{qs(d)}^*$ and $V_{tb} V_{ts(d)}^*$ are the products of the Cabibbo-Kobayashi-Maskawa (CKM) matrix elements. According to the scale μ , one can separate the effective Hamiltonian into two distinct parts: the Wilson coefficients C_i , and the local four-quark operators O_i . The local

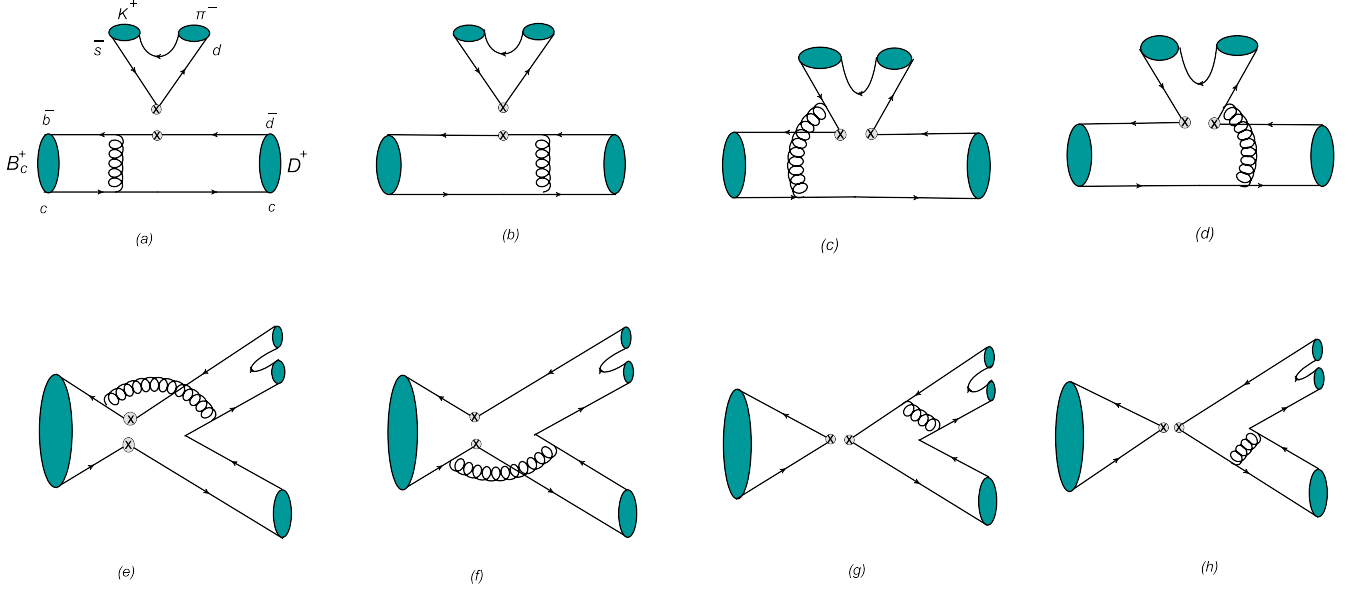


Figure 1: The leading order Feynman diagrams for the decay $B_c^+ \rightarrow K_0^{*0} D^+ \rightarrow K^+ \pi^- D^+$.

four-quark operators for the $b \rightarrow d$ transition are written as

$$\begin{aligned}
O_1^{(q)} &= (\bar{d}_i q_j)_{V-A} (\bar{q}_j b_i)_{V-A}, & O_2^{(q)} &= (\bar{d}_i q_i)_{V-A} (\bar{q}_j b_j)_{V-A}, \\
O_3 &= (\bar{d}_i b_i)_{V-A} \sum_q (\bar{q}_j q_j)_{V-A}, & O_4 &= (\bar{d}_i b_j)_{V-A} \sum_q (\bar{q}_j q_i)_{V-A}, \\
O_5 &= (\bar{d}_i b_i)_{V-A} \sum_q (\bar{q}_j q_j)_{V+A}, & O_6 &= (\bar{d}_i b_j)_{V-A} \sum_q (\bar{q}_j q_i)_{V+A}, \\
O_7 &= \frac{3}{2} (\bar{d}_i b_i)_{V-A} \sum_q e_q (\bar{q}_j q_j)_{V+A}, & O_8 &= \frac{3}{2} (\bar{d}_i b_j)_{V-A} \sum_q e_q (\bar{q}_j q_i)_{V+A}, \\
O_9 &= \frac{3}{2} (\bar{d}_i b_i)_{V-A} \sum_q e_q (\bar{q}_j q_j)_{V-A}, & O_{10} &= \frac{3}{2} (\bar{d}_i b_j)_{V-A} \sum_q e_q (\bar{q}_j q_i)_{V-A},
\end{aligned} \tag{18}$$

where i, j are the color indices and $V \pm A$ refer to the Lorentz structures $\gamma_\mu (1 \pm \gamma_5)$. Similarly, the local four-quark operators for the $b \rightarrow s$ transition can be obtained by replacing d with s in Eq. (18).

The typical Feynman diagrams at the leading order for the quasi-two-body decays $B_c \rightarrow K_0^{*0} D_{(s)} \rightarrow K \pi D_{(s)}$ are shown in Fig. 1, where we take the decay $B_c^+ \rightarrow K_0^{*0} D^+ \rightarrow K^+ \pi^- D^+$ as an example. We mark LL, LR, SP to denote the contributions from $(V-A)(V-A)$, $(V-A)(V+A)$ and $(S-P)(S+P)$ operators, respectively. The amplitudes from the factorizable emission diagrams Fig. 1(a) and 1(b) are given as

$$\begin{aligned}
\mathcal{F}_e^{LL} &= 2\sqrt{\frac{2}{3}}\pi f_{B_c} F_{K\pi} m_{B_c}^4 C_F \int_0^1 dx_3 \int_0^\infty b_1 b_3 db_1 db_3 \exp\left(-\frac{\omega_b^2 b_1^2}{2}\right) \phi_D(x_3, b_3) \\
&\times \left\{ [-\zeta + r(4\zeta - (\zeta + 1)r_b - 2(\zeta - 1)x_3) + 2r_b(1 - \zeta) - (1 - \zeta)^2 x_3] \right. \\
&\times \alpha_s(t_a) h(\alpha_e, \beta_a, b_1, b_3) \exp[-S_{ab}(t_a)] S_t(x_3) \\
&- [2r(\zeta(r_c + 1) + r_c - 1) - \zeta r_c] \\
&\times \alpha_s(t_b) h(\alpha_e, \beta_b, b_1, b_3) \exp[-S_{ab}(t_b)] S_t(r_c) \left. \right\}, \tag{19}
\end{aligned}$$

$$\mathcal{F}_e^{LL} = \mathcal{F}_e^{LR}, \tag{20}$$

$$\begin{aligned}
\mathcal{F}_e^{SP} &= -4\sqrt{\frac{2}{3}}\pi f_{B_c} F_{K\pi} m_{B_c}^4 C_F \sqrt{\zeta} \int_0^1 dx_3 \int_0^\infty b_1 b_3 db_1 db_3 \exp\left(-\frac{\omega_b^2 b_1^2}{2}\right) \phi_D(x_3, b_3) \\
&\times \left\{ [r(\zeta(1 - x_3) - 4r_b + x_3 + 1) - (1 - \zeta)(2 - r_b)] \right. \\
&\times \alpha_s(t_a) h(\alpha_e, \beta_a, b_1, b_3) \exp[-S_{ab}(t_a)] S_t(x_3) \\
&- [2r(1 - \zeta - 2r_c) + r_c(1 - \zeta)] \alpha_s(t_b) h(\alpha_e, \beta_b, b_1, b_3) \exp[-S_{ab}(t_b)] S_t(r_c) \left. \right\}, \tag{21}
\end{aligned}$$

where the mass ratios $r = m_D/m_{B_c}$, $r_b = m_b/m_{B_c}$. The hard function $h(\alpha_e, \beta_{a,b}, b_1, b_3)$, the hard scales $t_{a,b}$, the Sudakov factor $\exp[-S_{ab}(t)]$ and the threshold resummation factor $S_t(x)$ can be found in Appendix A. The amplitudes for the nonfactorizable emission diagrams Figs. 1(c) and 1(d) are written as

$$\begin{aligned} \mathcal{M}_e^{LL} &= -\frac{8}{3}\pi f_{B_c} m_{B_c}^4 C_F \int_0^1 dz dx_3 \int_0^\infty b_1 b db_1 db \exp\left(-\frac{\omega_b^2 b_1^2}{2}\right) \phi_D(x_3, b_3) \phi_0(z, s) \\ &\times \{[r(\zeta(r_c + 2z - x_3 - 1) + r_c + x_3 - 1) - r_c - z + 1] \\ &\times \alpha_s(t_c) h(\beta_c, \alpha_e, b_1, b_2) \exp[-S_{cd}(t_c)] \\ &- [r(\zeta(-r_c + 2z + x_3 - 1) - r_c - x_3 + 1) \\ &- 2\zeta(r_c + x_3 - 1) + 2r_c - z + x_3 - 1] \\ &\times \alpha_s(t_d) h(\beta_d, \alpha_e, b_1, b_2) \exp[-S_{cd}(t_d)]\}, \end{aligned} \quad (22)$$

$$\begin{aligned} \mathcal{M}_e^{LR} &= -\frac{8}{3}\pi f_{B_c} \sqrt{\zeta} m_{B_c}^4 C_F \int_0^1 dz dx_3 \int_0^\infty b_1 b db_1 db \exp\left(-\frac{\omega_b^2 b_1^2}{2}\right) \phi_D(x_3, b_1) \\ &\times \{[r(\phi_s(z, s)(-2r_c + z - x_3 + 2) + \zeta((\phi_s(z, s) - \phi_t(z, s))(x_3 - z)) + \phi_t(z, s)(x_3 - z)) \\ &+ (\zeta - 1)(\phi_s(z, s) + \phi_t(z, s))(r_c + z - 1)] \alpha_s(t_c) h(\beta_c, \alpha_e, b_1, b) \exp[-S_{cd}(t_c)] \\ &- [r(\phi_s(z, s)(2r_c - z + x_3 - 1) + \zeta(\phi_s(z, s) + \phi_t(z, s))(-z - x_3 + 1) + \phi_t(z, s)(z + x_3 - 1)) \\ &+ (\zeta - 1)(\phi_s(z, s) + \phi_t(z, s))(r_c - z)] \alpha_s(t_d) h(\beta_d, \alpha_e, b_1, b) \exp[-S_{cd}(t_d)]\}, \end{aligned} \quad (23)$$

$$\begin{aligned} \mathcal{M}_e^{SP} &= \frac{8}{3}\pi f_{B_c} m_{B_c}^4 C_F \int_0^1 dz dx_3 \int_0^\infty b_1 b db_1 db \exp\left(-\frac{\omega_b^2 b_1^2}{2}\right) \phi_D(x_3, b_1) \phi_0(z, b) \\ &\times \{[r(\zeta(r_c + 2z - x_3 - 1) + r_c + x_3 - 1) + 2\zeta(r_c + x_3 - 1) - 2r_c - z - x_3] \\ &\times \alpha_s(t_c) h(\beta_c, \alpha_e, b_1, b) \exp[-S_{cd}(t_c)] \\ &- [r(\zeta(r_c - 2z - x_3 + 1) + r_c + x_3 - 1) - r_c + z] \\ &\times \alpha_s(t_d) h(\beta_d, \alpha_e, b_1, b) \exp[-S_{cd}(t_d)]\}. \end{aligned} \quad (24)$$

It is noticed that the integration of b_3 has been performed using δ function $\delta(b_1 - b_3)$, leaving only integration of b_1 and b . The amplitudes from the nonfactorizable annihilation diagrams Figs. 1(e) and 1(f) are listed as

$$\begin{aligned} \mathcal{M}_a^{LL} &= \frac{8}{3}\pi f_{B_c} m_{B_c}^4 C_F \int_0^1 dz dx_3 \int_0^\infty b_1 b_3 db_1 db_3 \exp\left(-\frac{\omega_b^2 b_1^2}{2}\right) \phi_D(x_3, b_3) \\ &\times \left\{ [r\sqrt{\zeta}(\phi_s(z, s)(-4r_b - 2r_c - z - x_3 + 2) + \phi_t(z, s)(x_3 - z) \right. \\ &\quad \left. + \zeta(\phi_s(z, s) - \phi_t(z, s))(x_3 - z)) + \phi_0(z, s)(r_b(\zeta - 1) - r_c - z + 1)] \right. \\ &\times \alpha_s(t_e) h(\beta_e, \alpha_a, b_1, b_3) \exp[-S_{ef}(t_e)] \\ &\quad \left. + [r\sqrt{\zeta}(\phi_s(z, s)(2r_c + z + x_3) + \phi_t(z, s)(x_3 - z) \right. \\ &\quad \left. + \zeta(\phi_s(z, s) + \phi_t(z, s))(z - x_3)) + \phi_0(z, s)(x_3 - \zeta(r_c - 2z + 2x_3))] \right. \\ &\quad \left. \times \alpha_s(t_f) h(\beta_f, \alpha_a, b_1, b_3) \exp[-S_{ef}(t_f)] \right\}, \end{aligned} \quad (25)$$

$$\begin{aligned} M_a^{LR} &= \frac{8}{3}\pi f_{B_c} m_{B_c}^4 C_F \int_0^1 dz dx_3 \int_0^\infty b_1 b_3 db_1 db_3 \exp\left(-\frac{\omega_b^2 b_1^2}{2}\right) \phi_D(x_3, b_3) \\ &\times [r((\zeta + 1)(-r_b + r_c - x_3 - 1) + 2(z + x_3))\phi_0(z, s) \\ &\quad + \sqrt{\zeta}(1 - \zeta)(\phi_s(z, s) + \phi_t(z, s))(r_b - r_c - z + 1)] \\ &\times \alpha_s(t_e) h(\beta_e, \alpha_a, b_1, b_3) \exp[-S_{ef}(t_e)] \\ &\quad + [r((\zeta + 1)(2r_c - x_3) - 2(z - x_3))\phi_0(z, s) \\ &\quad + \sqrt{\zeta}(1 - \zeta)(\phi_s(z, s) + \phi_t(z, s))(-2r_c + z)] \\ &\times \alpha_s(t_f) h(\beta_f, \alpha_a, b_1, b_3) \exp[-S_{ef}(t_f)]. \end{aligned} \quad (26)$$

The amplitudes from the factorizable annihilation diagrams Figs. 1(g) and 1(h) are given as

$$\begin{aligned}
\mathcal{F}_a^{LL} &= 8\pi f_{B_c} m_{B_c}^4 C_F \int_0^1 dz dx_3 \int_0^\infty bb_3 db db_3 \phi_D(x_3, b_3) \\
&\times \left\{ \left[2r \left(\zeta^{3/2} (x_3 - 1) - \sqrt{\zeta} (x_3 + 1) \right) \phi_s(z, s) + (\zeta (2x_3 - 1) - x_3) \phi_0(z, s) \right] \right. \\
&\times \alpha_s(t_g) h(\alpha_a, \beta_g, b_2, b_3) \exp[-S_{gh}(t_g)] S_t(x_3) \\
&- \left[2r \left(r_c(\zeta + 1) \phi_0(z, s) + \zeta^{3/2} (z - 1) (\phi_t(z, s) - \phi_s(z, s)) \right. \right. \\
&- 2\sqrt{\zeta} ((1 + z) \phi_s(z, s) - (1 - z) \phi_t(z, s))] + \sqrt{\zeta} (\zeta - 1) r_c (\phi_t(z, s) - \phi_s(z, s)) \\
&\left. \left. + (\zeta - 1) z \phi_0(z, s) \right] \alpha_s(t_h) h(\alpha_a, \beta_h, b_3, b_2) \exp[-S_{gh}(t_h)] S_t(z) \right\}, \tag{27}
\end{aligned}$$

$$\begin{aligned}
\mathcal{F}_a^{SP} &= 16\pi f_{B_c} m_{B_c}^4 C_F \int_0^1 dz dx_3 \int_0^\infty bb_3 db db_3 \phi_D(x_3, b_3) \\
&\left\{ \left[-2\sqrt{\zeta} (\zeta - 1) \phi_s(z, s) + r \phi_0(z, s) (\zeta (2 - x_3) + x_3) \right] \right. \\
&\times \alpha_s(t_g) h_e(\alpha_a, \beta_g, b_2, b_3) \exp[-S_{gh}(t_g)] S_t(x_3) \\
&- \left[2r \left(2\sqrt{\zeta} r_c \phi_s(z, s) - (\zeta (2z - 1) + 1) \phi_0(z, s) \right) \right. \\
&- (\zeta - 1) r_c \phi_0(z, s) + \sqrt{\zeta} (\zeta - 1) z (\phi_s(z, s) - \phi_t(z, s)) \left. \right] \\
&\left. \times \alpha_s(t_h) h_e(\alpha_a, \beta_h, b_3, b_2) \exp[-S_{gh}(t_h)] S_t(z) \right\}. \tag{28}
\end{aligned}$$

By combining the amplitudes from the different Feynman diagrams, the total decay amplitudes for the quasi-two-body decays $B_c \rightarrow K_0^* D_{(s)} \rightarrow K \pi D_{(s)}$ can be written as

$$\begin{aligned}
\mathcal{A}(B_c^+ \rightarrow K_0^{*+} D^0 \rightarrow K^0 \pi^+ D^0) &= V_{us} V_{ub}^* [a_1 \mathcal{F}_e^{LL} + C_1 \mathcal{M}_e^{LL}] + V_{cs} V_{cb}^* [a_1 \mathcal{F}_a^{LL} + C_1 \mathcal{M}_a^{LL}] \\
&- V_{ts} V_{tb}^* [(C_3 + C_9) (\mathcal{M}_e^{LL} + \mathcal{M}_a^{LL}) + (C_5 + C_7) (\mathcal{M}_e^{LR} + \mathcal{M}_a^{LR}) \\
&+ (C_4 + \frac{1}{3} C_3 + C_{10} + \frac{1}{3} C_9) (\mathcal{F}_a^{LL} + \mathcal{F}_e^{LL}) \\
&+ (C_6 + \frac{1}{3} C_5 + C_8 + \frac{1}{3} C_7) (\mathcal{F}_a^{SP} + \mathcal{F}_e^{SP})], \tag{29}
\end{aligned}$$

$$\begin{aligned}
\mathcal{A}(B_c^+ \rightarrow K_0^{*0} D^+ \rightarrow K^+ \pi^- D^+) &= V_{cs} V_{cb}^* [a_1 \mathcal{F}_a^{LL} + C_1 \mathcal{M}_a^{LL}] - V_{ts} V_{tb}^* \left[(C_3 - \frac{1}{2} C_9) \mathcal{M}_e^{LL} \right. \\
&+ (C_3 + C_9) \mathcal{M}_a^{LL} + (C_5 - \frac{1}{2} C_7) \mathcal{M}_e^{LR} + (C_5 + C_7) \mathcal{M}_a^{LR} \\
&+ (C_4 + \frac{1}{3} C_3 + C_{10} + \frac{1}{3} C_9) \mathcal{F}_a^{LL} \\
&+ (C_4 + \frac{1}{3} C_3 - \frac{1}{2} C_{10} - \frac{1}{6} C_9) \mathcal{F}_e^{LL} + (C_6 + \frac{1}{3} C_5 - \frac{1}{2} C_8 \\
&- \frac{1}{6} C_7) \mathcal{F}_e^{SP} + (C_6 + \frac{1}{3} C_5 + C_8 + \frac{1}{3} C_7) \mathcal{F}_a^{SP} \left. \right], \tag{30}
\end{aligned}$$

$$\begin{aligned}
\mathcal{A}(B_c^+ \rightarrow \bar{K}_0^{*0} D_s^+ \rightarrow K^- \pi^+ D_s^+) &= V_{cd} V_{cb}^* [a_1 \mathcal{F}_a^{LL} + C_1 \mathcal{M}_a^{LL}] - V_{td} V_{tb}^* \left[(C_3 - \frac{1}{2} C_9) \mathcal{M}_e^{LL} \right. \\
&+ (C_3 + C_9) \mathcal{M}_a^{LL} + (C_5 - \frac{1}{2} C_7) \mathcal{M}_e^{LR} + (C_5 + C_7) \mathcal{M}_a^{LR} \\
&+ (C_4 + \frac{1}{3} C_3 + C_{10} + \frac{1}{3} C_9) \mathcal{F}_a^{LL} \\
&+ (C_4 + \frac{1}{3} C_3 - \frac{1}{2} C_{10} - \frac{1}{6} C_9) \mathcal{F}_e^{LL} + (C_6 + \frac{1}{3} C_5 - \frac{1}{2} C_8 \\
&- \frac{1}{6} C_7) \mathcal{F}_e^{SP} + (C_6 + \frac{1}{3} C_5 + C_8 + \frac{1}{3} C_7) \mathcal{F}_a^{SP} \left. \right]. \tag{31}
\end{aligned}$$

Using these total decay amplitudes, one can calculate the differential decay rate with the following formula

$$\frac{d\mathcal{B}r}{d\omega^2} = \tau_{B_c} \frac{|\vec{p}_1| |\vec{p}_3|}{64\pi^3 m_{B_c}^3} |\mathcal{A}|^2, \quad (32)$$

where τ_{B_c} is the mean lifetime of B_c meson, the kinematic variables $|\vec{p}_1|$ and $|\vec{p}_3|$ denote the magnitudes of the daughter meson (K or π) and the bachelor meson $D_{(s)}$ momenta in the center-of-mass frame of the $K\pi$ pair,

$$\begin{aligned} |\vec{p}_1| &= \frac{1}{2} \sqrt{\left[(m_K^2 - m_\pi^2)^2 - 2(m_K^2 + m_\pi^2)w^2 + w^4 \right] / w^2}, \\ |\vec{p}_3| &= \frac{1}{2} \sqrt{\left[(m_{B_c}^2 - m_D^2)^2 - 2(m_{B_c}^2 + m_D^2)w^2 + w^4 \right] / w^2}. \end{aligned} \quad (33)$$

III. NUMERICAL RESULTS

The input parameters in our numerical calculations are listed as following (the QCD scale, the masses, the decay constants and the widths are in units of GeV, the B_c meson lifetime is in units of ps) [7, 49]

$$\begin{aligned} \Lambda_{QCD} &= 0.25, m_{B_c^+} = 6.274, m_b = 4.8, m_{K^\pm} = 0.494, m_{K^0} = 0.498, m_{\pi^\pm} = 0.140, m_{\pi^0} = 0.135, \\ m_{K_0^*(1430)} &= 1.425 \pm 0.050, m_{K_0^*(1950)} = 1.945 \pm 0.010, \Gamma_{K_0^*(1430)} = 0.270 \pm 0.080, \\ \Gamma_{K_0^*(1950)} &= 0.100 \pm 0.040 \text{ (} 0.201 \pm 0.034 \text{)}, f_{B_c} = 0.489, \tau_{B_c} = 0.51. \end{aligned} \quad (34)$$

As to the Cabibbo-Kobayashi-Maskawa (CKM) matrix elements, we employ the Wolfenstein parametrization with the inputs [49]

$$\begin{aligned} \lambda &= 0.22500 \pm 0.00067, \quad A = 0.826_{-0.015}^{+0.018}, \\ \bar{\rho} &= 0.159 \pm 0.010, \quad \bar{\eta} = 0.348 \pm 0.010. \end{aligned} \quad (35)$$

By using the differential branching ratio in Eq.(32) and the squared amplitudes in Eqs.(29)-(31), integrating over the full $K\pi$ invariant mass region $(m_K + m_\pi) \leq \omega \leq (M_{B_c} - m_{D_{(s)}})$, we can obtain the branching ratios for these quasi-two-body decays $B_c^+ \rightarrow K_0^* D_{(s)} \rightarrow K\pi D_{(s)}$ by using two different parametrizations mentioned in previous section, i.e., the LASS line shape and the RBW function, to the intermediate resonances. In view of the large deviations for the measurements about the $K_0^*(1950)$ decay width between the LASS [7] and BaBar [12], we take two width values $\Gamma_{K_0^*(1950)} = 0.100 \pm 0.040$ GeV [49] and $\Gamma_{K_0^*(1950)} = 0.201 \pm 0.034$ GeV [7] in our calculations for comparison. The results are listed in Table 1, where the first error is from the B_c meson shape parameter uncertainty $\omega_{B_c} = 0.6 \pm 0.05$ GeV, the following two errors come from the Gegenbauer moments in the $K\pi$ pair distribution amplitudes $a_1 = -0.57 \pm 0.13$, $a_2 = -0.42 \pm 0.22$, and the last one is induced by varying the QCD scale $\Lambda_{QCD} = 0.25 \pm 0.05$ GeV from the next-to-leading-order (NLO) effect in the PQCD approach. These results are sensitive to the value of the QCD scale Λ_{QCD} , which indicate that the NLO contributions maybe play an important role in these decays. Another important uncertainty is from the Gegenbauer coefficient $a_2 = -0.42 \pm 0.22$. Some comments are in order:

Table 1: Branching ratios of the quasi-two-body decays $B_c^+ \rightarrow K_0^*(1430, 1950)D_{(s)} \rightarrow K\pi D_{(s)}$ within the LASS and the RBW parametrizations.

Decay modes	$\Gamma_{K_0^*}$ (GeV)	LASS	RBW
$B_c^+ \rightarrow K^{*+}(1430)D^0 \rightarrow K^0\pi^+D^0$	0.270	$(2.71_{-0.04}^{+0.05+0.20+0.91+1.28} - 0.21 - 0.66 - 0.55) \times 10^{-4}$	$(0.61_{-0.02}^{+0.02+0.05+0.33+0.80} - 0.03 - 0.21 - 0.00) \times 10^{-4}$
$B_c^+ \rightarrow K^{*0}(1430)D^+ \rightarrow K^+\pi^-D^+$	0.270	$(3.06_{-0.04}^{+0.04+0.23+0.97+1.63} - 0.24 - 0.00 - 0.69) \times 10^{-4}$	$(0.64_{-0.02}^{+0.02+0.05+0.33+0.88} - 0.03 - 0.21 - 0.00) \times 10^{-4}$
$B_c^+ \rightarrow \bar{K}^{*0}(1430)D_s^+ \rightarrow K^-\pi^+D_s^+$	0.270	$(2.04_{-0.03}^{+0.04+0.16+0.62+1.10} - 0.15 - 0.47 - 0.45) \times 10^{-5}$	$(0.48_{-0.01}^{+0.01+0.04+0.25+0.68} - 0.04 - 0.16 - 0.00) \times 10^{-5}$
$B_c^+ \rightarrow K^{*+}(1950)D^0 \rightarrow K^0\pi^+D^0$	0.100	$(7.76_{-0.12}^{+0.12+0.22+3.11+1.63} - 0.19 - 2.41 - 1.30) \times 10^{-5}$	$(2.73_{-0.05}^{+0.04+0.02+1.19+1.91} - 0.04 - 1.00 - 2.36) \times 10^{-5}$
$B_c^+ \rightarrow K^{*+}(1950)D^0 \rightarrow K^0\pi^+D^0$	0.201	$(1.99_{-0.03}^{+0.03+0.06+0.84+0.19} - 0.06 - 0.65 - 0.89) \times 10^{-5}$	$(1.31_{-0.02}^{+0.02+0.00+0.57+0.77} - 0.02 - 0.48 - 1.03) \times 10^{-5}$
$B_c^+ \rightarrow K^{*0}(1950)D^+ \rightarrow K^+\pi^-D^+$	0.100	$(7.80_{-0.14}^{+0.14+0.23+3.39+2.35} - 0.16 - 2.38 - 0.54) \times 10^{-5}$	$(2.55_{-0.05}^{+0.06+0.04+1.42+2.13} - 0.02 - 0.94 - 2.18) \times 10^{-5}$
$B_c^+ \rightarrow K^{*0}(1950)D^+ \rightarrow K^+\pi^-D^+$	0.201	$(2.01_{-0.04}^{+0.04+0.08+0.92+1.10} - 0.06 - 0.63 - 0.05) \times 10^{-5}$	$(1.27_{-0.03}^{+0.03+0.01+0.66+0.92} - 0.00 - 0.46 - 0.98) \times 10^{-5}$
$B_c^+ \rightarrow \bar{K}^{*0}(1950)D_s^+ \rightarrow K^-\pi^+D_s^+$	0.100	$(5.47_{-0.12}^{+0.12+0.16+2.21+1.79} - 0.05 - 1.59 - 0.41) \times 10^{-6}$	$(1.82_{-0.05}^{+0.04+0.72+0.97+1.52} - 0.00 - 0.62 - 1.54) \times 10^{-6}$
$B_c^+ \rightarrow \bar{K}^{*0}(1950)D_s^+ \rightarrow K^-\pi^+D_s^+$	0.201	$(1.37_{-0.03}^{+0.03+0.06+0.59+0.83} - 0.02 - 0.41 - 0.03) \times 10^{-6}$	$(0.91_{-0.02}^{+0.02+0.03+0.44+0.67} - 0.00 - 0.30 - 0.70) \times 10^{-6}$

1. For the decays with $K_0^*(1430)$ involved there exists a significant difference in the branching ratios obtained using these two different parameterization schemes to the time-like from factor. If taken the RBW model with only the resonance contribution being considered, the corresponding branching ratios will be much smaller than those obtained using the LASS form, where both the resonance and nonresonance contributions are included. For example, $\mathcal{B}r(B_c^+ \rightarrow \bar{K}_0^{*0}(1430)D_s^+ \rightarrow K^-\pi^+D_s^+)$ under the RBW parameterization is only one fifth of that under the LASS form. Such large difference should be detected by the future experiments, then one can clarify which parameterization scheme is more reasonable. The branching ratios of the decays with $D^{0,+}$ mesons involved are about one order larger than that of the decay with D_s^+ involved, this is mainly because that the CKM element $V_{cs}(V_{ts})$ associated with the former is about 5 times of $V_{cd}(V_{td})$ associated with the latter. For the decay $B_c^+ \rightarrow K_0^{*+}(1430)D^0 \rightarrow K^0\pi^+D^0$, the main contributions come from the annihilation type amplitudes with the tree operators F_a^{LL} and M_a^{LL} . Such contributions are much larger than another kind of tree contributions associated with $V_{us}V_{ub}^*$. Although the values of the CKM matrix elements $V_{cb}^*V_{cs}$ and $V_{tb}^*V_{ts}$ are close to each other, the contributions from the penguin operators are small and only about 2% because of the smallness of the Wilson coefficients. These characters are very different with the case of the decay $B_c^+ \rightarrow K^{*+}(892)D^0 \rightarrow K^0\pi^+D^0$ [50].
2. As we know, the narrow resonances, such as $K^*(892)$, can be well described by the RBW model, which has been adopted extensively in experimental analysis. While it is failed to describe the broad resonances, such as $K_0^*(1430)$, which is usually considered to be interfere strongly with a slowly varying nonresonant contribution [6]. On the experimental side, the LASS line shape was proposed to describe the combined contributions from the resonant and non-resonant components [7]. As to the decays with $K_0^*(1430)$ involved, the resonant contributions come from the second term in the LASS parameterization shown in Eq. (15) are only about 20% of the total branching ratios. It is similar to the case of the decays $B \rightarrow KKK$, where the nonresonant background are dominant. For example, the resonant fraction is about 10% in the channel $B^0 \rightarrow K^+K^-K^0$ [51]. In the decays $B \rightarrow K_0^*(1430)D \rightarrow K\pi D$, the resonant contributions are estimated to be 50% [11].
3. For the decays with $K_0^*(1950)$ involved, besides two parametrization schemes we use two width values $\Gamma_{K_0^*(1950)} = 0.100, 0.201$ GeV in our calculations. In Table 1, one can find that the differences of the branching ratios between these two parameterization schemes are not very large for $\Gamma_{K_0^*(1950)} = 0.201$ GeV. The branching ratios obtained in the LASS (RBW) parametrization are (not) sensitive to the values of $\Gamma_{K_0^*(1950)}$. On the other hand, one can find that the proportions of the resonant contributions in the decay channels containing $K_0^*(1950)$ are larger compared to those in the decays with $K_0^*(1430)$ involved. The resonant contributions are more than 30%(60%) with $\Gamma_{K_0^*(1950)} = 0.100(0.201)$ GeV. In addition, there exist destructive interferences with different strengths between the resonant and nonresonant contributions in these considered decays $B_c \rightarrow K_0^*(1430, 1950)D_{(s)}$.

Under the so-called narrow width approximation (NWA) one can extract the branching fraction of the two-body decay $B_c \rightarrow RP$ from that of the quasi-two-body one $B_c \rightarrow RP \rightarrow P_1P_2P$, that is

$$\Gamma(B_c \rightarrow RP \rightarrow P_1P_2P) = \Gamma(B_c \rightarrow RP) \mathcal{B}r(R \rightarrow P_1P_2). \quad (36)$$

Here the strong decay $R \rightarrow P_1P_2$ represents $K_0^*(1430) \rightarrow K\pi$ and $K_0^*(1950) \rightarrow K\pi$, whose branching ratios are given as 0.93 ± 0.10 and 0.52 ± 0.14 [49], respectively, and the branching ratios of the decays $K_0^{*0}(1430, 1950) \rightarrow K^+\pi^-$ and $K_0^{*+}(1430, 1950) \rightarrow K^0\pi^+$ can be obtained from the isospin conservation, namely

$$\frac{\Gamma(K_0^{*0}(1430, 1950) \rightarrow K^+\pi^-)}{\Gamma(K_0^{*0}(1430, 1950) \rightarrow K\pi)} = \frac{\Gamma(K_0^{*+}(1430, 1950) \rightarrow K^0\pi^+)}{\Gamma(K_0^{*+}(1430, 1950) \rightarrow K\pi)} = 2/3. \quad (37)$$

In Eq. (36), R refers to an intermediate resonant state with the zero width limit $\Gamma_R \rightarrow 0$. While the scalar resonances $K_0^*(1430, 1950)$ considered here have broad decay widths, one should take into account the finite-width effects, which are defined as η_R . Here we take $\eta_{K_0^*(1430)}$ within the RBW parameterization as an example,

$$\begin{aligned} \eta_{K_0^*(1430)} &= \frac{\Gamma(B_c \rightarrow K_0^*(1430)D_{(s)} \rightarrow K\pi D_{(s)})}{\Gamma(B_c \rightarrow K_0^*(1430)D_{(s)}) \times \mathcal{B}(K_0^* \rightarrow K\pi)} \\ &\approx \frac{m_{K_0^*(1430)}^2}{4\pi m_{B_c}} \frac{\Gamma_{K_0^*(1430)}}{q_{D_{(s)}} q_0} \int_{(m_K+m_\pi)^2}^{(m_{B_c}-m_{D_{(s)}})^2} ds \frac{\lambda^{1/2}(m_{B_c}^2, s, m_{D_{(s)}}^2) \lambda^{1/2}(s, m_K^2, m_\pi^2)}{s \left((s - m_{K_0^*(1430)}^2)^2 + (m_{K_0^*(1430)} \Gamma_{K_0^*(1430)}(s))^2 \right)}, \end{aligned} \quad (38)$$

where $\lambda(a, b, c) = a^2 + b^2 + c^2 - 2ab - 2ac - 2bc$, and $q_{D_{(s)}}$ refers to the magnitude momentum of the bachelor meson $D_{(s)}$ and is given as

$$q_{D_{(s)}} = \frac{1}{2} \sqrt{\left[\left(m_{B_c}^2 - m_{D_{(s)}}^2 \right)^2 - 2 \left(m_{B_c}^2 + m_{D_{(s)}}^2 \right) s + s^2 \right]} / s, \quad (39)$$

with s being fixed at $m_{K_0^*(1430)}^2$. For our considered decays, the values of η_R are calculated as $\eta_{K_0^*(1430)} = 0.90$ and $\eta_{K_0^*(1950)} = 0.94(0.97)$ with $\Gamma_{K_0^*(1950)} = 0.201(0.100)$ GeV. As to $\eta_{K_0^*(1430)}$, it was also discussed in Ref. [52], where its values were given as $\eta_{K_0^*(1430)}^{\text{QCDF}} = 0.83$ and $\eta_{K_0^*(1430)}^{\text{EXPP}} = 1.10$ ². The former was calculated within the QCD factorization (QCDF) framework, and the latter was abstracted from the data. It is obviously that our value of $\eta_{K_0^*(1430)}$ is larger than the QCDF result, but smaller than that abstracted from the data. After considering the decay width effects, the branching ratios for the two-body decays $B_c \rightarrow K_0^* D_{(s)}$ can be related to our considered decays from the following formula

$$Br(B_c \rightarrow K_0^* D_{(s)} \rightarrow K\pi D_{(s)}) = \eta_{K_0^*} \cdot Br(B_c \rightarrow K_0^* D_{(s)}) \cdot Br(K_0^* \rightarrow K\pi). \quad (40)$$

Table 2: The branching ratios of the (quasi-)two-body decays $B_c \rightarrow K_0^*(1430)D_{(s)} (\rightarrow K\pi D_{(s)})$ within the LASS and the RBW parametrization schemes. For comparison, we also list the previous PQCD calculations in the two-body framework under SII as given in Ref. [16].

Decay modes	scheme	Quasi-two-body	Two-body	PQCD (SII) [16]
$B_c^+ \rightarrow K_0^{*+}(1430)D^0 (\rightarrow K^0\pi^+D^0)$	LASS	$(2.71_{-0.89}^{+1.58}) \times 10^{-4}$	$(3.97_{-1.30}^{+2.32}) \times 10^{-4}$	$(4.58 \pm 2.42) \times 10^{-4}$
	RBW	$(0.61_{-0.21}^{+0.94}) \times 10^{-4}$	$(0.89_{-0.31}^{+1.37}) \times 10^{-4}$	
$B_c^+ \rightarrow K_0^{*0}(1430)D^+ (\rightarrow K^+\pi^-D^+)$	LASS	$(3.06_{-0.73}^{+1.91}) \times 10^{-4}$	$4.48_{-1.07}^{+2.80} \times 10^{-4}$	$(4.81_{-2.73}^{+2.44}) \times 10^{-4}$
	RBW	$(0.64_{-0.22}^{+0.94}) \times 10^{-4}$	$(0.94_{-0.32}^{+1.38}) \times 10^{-4}$	
$B_c^+ \rightarrow \bar{K}_0^{*0}(1430)D_s^+ (\rightarrow K^-\pi^+D_s^+)$	LASS	$(2.04_{-0.67}^{+1.27}) \times 10^{-5}$	$(2.99_{-0.98}^{+1.86}) \times 10^{-5}$	$(2.79_{-1.31}^{+1.70}) \times 10^{-5}$
	RBW	$(0.48_{-0.17}^{+0.73}) \times 10^{-5}$	$(0.70_{-0.25}^{+1.07}) \times 10^{-5}$	

Table 3: Same as Table 2 except for the (quasi-)two-body decays $B_c \rightarrow K_0^*(1950)D_{(s)} (\rightarrow K\pi D_{(s)})$.

Decay Modes	$\Gamma_{K_0^*(1950)}$	Quasi-two-body (LASS)	Two-body(LASS)	Quasi-two-body(RBW)	Two-body(RBW)
$B_c^+ \rightarrow K_0^{*+}(1950)D^0$ ($\rightarrow K^0\pi^+D^0$)	0.100GeV	$7.76_{-2.74}^{+3.52} \times 10^{-5}$	$1.77_{-0.63}^{+0.80} \times 10^{-4}$	$2.73_{-2.56}^{+2.25} \times 10^{-5}$	$5.42_{-5.08}^{+4.47} \times 10^{-5}$
	0.201GeV	$1.99_{-1.10}^{+0.86} \times 10^{-5}$	$4.54_{-2.46}^{+1.92} \times 10^{-5}$	$1.31_{-1.14}^{+0.96} \times 10^{-5}$	$2.99_{-2.60}^{+2.19} \times 10^{-5}$
$B_c^+ \rightarrow K_0^{*0}(1950)D^+$ ($\rightarrow K^+\pi^-D^+$)	0.100GeV	$7.80_{-2.45}^{+4.13} \times 10^{-5}$	$1.78_{-0.56}^{+0.94} \times 10^{-4}$	$2.55_{-2.37}^{+2.56} \times 10^{-5}$	$5.82_{-5.41}^{+5.84} \times 10^{-5}$
	0.201GeV	$2.01_{-0.63}^{+0.93} \times 10^{-5}$	$4.59_{-1.44}^{+2.12} \times 10^{-5}$	$1.27_{-1.08}^{+1.13} \times 10^{-5}$	$2.90_{-2.47}^{+2.58} \times 10^{-5}$
$B_c^+ \rightarrow \bar{K}_0^{*0}(1950)D_s^+$ ($\rightarrow K^-\pi^+D_s^+$)	0.100GeV	$5.47_{-1.65}^{+2.85} \times 10^{-6}$	$1.25_{-0.38}^{+0.65} \times 10^{-5}$	$1.82_{-1.66}^{+1.94} \times 10^{-6}$	$4.16_{-3.79}^{+4.43} \times 10^{-6}$
	0.201GeV	$1.37_{-0.41}^{+1.02} \times 10^{-6}$	$3.13_{-0.94}^{+2.33} \times 10^{-6}$	$0.91_{-0.76}^{+0.80} \times 10^{-6}$	$2.08_{-1.74}^{+1.83} \times 10^{-6}$

The corresponding results are listed in Tables 2 and 3, where the errors are the same with those given in Table 1. In Table 2, we also present the previous PQCD results calculated in the two-body framework [16], where $K_0^*(1430)$ is considered as the lowest lying $q\bar{s}$ state (SII) and the first excited $q\bar{s}$ state (SI), respectively. The branching

²The definition of η_R and that used in Ref. [52] are the inverse of each other.

ratios of the two-body decays $B_c \rightarrow K_0^*(1430)D_{(s)}$ obtained from the NWA with the decay width effects considered under the LASS parameterization are consistent well with the previous PQCD results calculated in SII, while the branching ratios under the RBW parameterization are much smaller than the previous results given in the two scenarios. The scalar meson $K_0^*(1430)$ has also been studied in the $B_{(s)}$ decays by many authors [39, 53], where the SII explanation is more favored. If the decays $B_c \rightarrow K_0^*(1430)D_{(s)}$ can be detected by the future experiments with the large branching ratios at the order of $10^{-5} \sim 10^{-4}$, one can speculate that the LASS parameterization is more preferable to describe the $K_0^*(1430)$.

Now we turn to the evaluations of the direct CP violation for the these considered decays, which are induced by the interference between the tree and penguin amplitudes and can be defined as

$$A_{CP} = \frac{\Gamma(B_c^- \rightarrow \bar{f}) - \Gamma(B_c^+ \rightarrow f)}{\Gamma(B_c^- \rightarrow \bar{f}) + \Gamma(B_c^+ \rightarrow f)}. \quad (41)$$

Here \bar{f} is the CP conjugated final state of f . The numerical results are listed in Table 4. It is obvious that these results are not sensitive to the parameters in the DAs, but suffer from large uncertainties due to the QCD scale Λ_{QCD} , which can be reduced by including the high order corrections. From the numerical results, we find the following points:

Table 4: The direct CP violations (%) of the decays $B_c \rightarrow K_0^*D_{(s)}(\rightarrow K\pi D_{(s)})$, where the errors are the same with those given in Table 1. The previous PQCD results (SII) [16] within the two-body framework are also listed for comparison.

Decay modes	LASS	RBW	PQCD (SII) [16]
$B_c^+ \rightarrow K^{*+}(1430)D^0(\rightarrow K^0\pi^+D^0)$	$0.58^{+0.01+0.36+0.86+0.65}_{-0.01-0.32-0.71-2.16}$	$-1.84^{+0.23+0.71+1.39+2.83}_{-0.22-0.67-0.59-0.74}$	$0.24^{+0.14}_{-0.14}$
$B_c^+ \rightarrow K^{*0}(1430)D^+(\rightarrow K^+\pi^-D^+)$	$0.09^{+0.00+0.02+0.03+0.14}_{-0.00-0.01-0.04-0.09}$	$0.29^{+0.01+0.03+0.02+0.02}_{-0.01-0.04-0.09-0.34}$	0.0
$B_c^+ \rightarrow \bar{K}^{*0}(1430)D_s^+(\rightarrow K^-\pi^+D_s^+)$	$-5.48^{+0.31+0.48+0.25+1.93}_{-0.31-0.37-0.00-2.46}$	$-9.71^{+0.58+1.16+0.72+6.61}_{-0.58-0.94-0.00-0.00}$	$-3.14^{+1.72}_{-2.17}$
$B_c^+ \rightarrow K^{*+}(1950)D^0(\rightarrow K^0\pi^+D^0)$	$-1.29^{+0.12+0.41+0.38+0.16}_{-0.12-0.35-0.22-0.48}$	$-2.40^{+0.19+0.50+0.17+0.91}_{-0.20-0.45-0.19-2.14}$	
$B_c^+ \rightarrow K^{*0}(1950)D^+(\rightarrow K^+\pi^-D^+)$	$0.24^{+0.01+0.04+0.00+0.00}_{-0.01-0.04-0.01-0.15}$	$0.37^{+0.01+0.05+0.06+0.22}_{-0.01-0.06-0.05-0.15}$	
$B_c^+ \rightarrow \bar{K}^{*0}(1950)D_s^+(\rightarrow K^-\pi^+D_s^+)$	$-6.37^{+0.26+1.03+0.58+1.89}_{-0.26-0.88-0.46-0.00}$	$-7.26^{+0.21+1.42+1.10+2.15}_{-0.20-1.17-1.07-7.19}$	

1. The direct CP violations for these considered decays predicted by using the LASS parametrization are closer to the previous PQCD calculations under the two-body framework compared to those obtained under the RBW form. It indicates that the LASS parametrization is more suitable to describe the scalar meson $K_0^*(1430)$. Especially for the decay $B_c^+ \rightarrow K_0^{*+}(1430)D^0 \rightarrow K^0\pi^+D^0$, its direct CP violation is minus under the RBW parametrization, while the sign will be flipped by the contribution from the nonresonant component in the LASS form.
2. As to the decays with the scalar meson $K_0^*(1950)$ involved, their direct CP violations are similar to those of the corresponding channels with $K_0^*(1430)$ involved. This is consistent with our expectation that these two scalar mesons should have similar properties in the B_c meson decays, while there seem to exist some differences between these two mesons: the CP violations for the decays involving $K_0^*(1950)$ between these two parametrizations are close to each other, indicating that the effect from the nonresonant contribution may not be so serious as that for the case of decays involving $K_0^*(1430)$.
3. The amplitudes of the decay $B_c^+ \rightarrow \bar{K}_0^{*0}D_s^+ \rightarrow K^-\pi^+D_s^+$ can be obtained from those of the channel $B_c^+ \rightarrow K_0^{*0}D^+ \rightarrow K^+\pi^-D^+$ by replacing $D^+(V_{ts}, V_{cs})$ with $D_s^+(V_{td}, V_{cd})$. The total decay amplitudes for these two decays can be rewritten as

$$\mathcal{A} = V_{cb}^*V_{cq}T - V_{tb}^*V_{tq}P = V_{cb}^*V_{cq}T \left[1 + ze^{i(\alpha+\delta)} \right], \quad (42)$$

where T and P are the tree and penguin amplitudes, α and δ are the weak and strong phases, respectively. The parameters z and α are defined as

$$z = \left| \frac{V_{tb}^*V_{tq}P}{V_{cb}^*V_{cq}T} \right|, \quad \alpha = \arg \left[-\frac{V_{tb}^*V_{tq}}{V_{cb}^*V_{cq}} \right], \quad (43)$$

with $q = d(s)$ for the decay $B_c^+ \rightarrow \bar{K}_0^{*0} D_s^+ \rightarrow K^- \pi^+ D_s^+$ ($B_c^+ \rightarrow K_0^{*0} D^+ \rightarrow K^+ \pi^- D^+$). Then the direct CP asymmetry is written as

$$A_{CP} = \frac{2z \sin \alpha \sin \delta}{z^2 + 1 + 2 \cos \alpha \cos \delta}. \quad (44)$$

As the weak phases are measured as $\arg \left[-\frac{V_{ub}^* V_{td}}{V_{cb}^* V_{cd}} \right] \sim -0.40$ and $\arg \left[-\frac{V_{ub}^* V_{ts}}{V_{cb}^* V_{cs}} \right] \sim 0.02$ [49], their corresponding sine values are about -0.39 and 0.02. So one can find that the size of A_{CP} ($B_c \rightarrow \bar{K}_0^{*0} D_s^+ \rightarrow K^- \pi^+ D_s^+$) is larger than that of A_{CP} ($B_c^+ \rightarrow K_0^{*0} D^+ \rightarrow K^+ \pi^- D^+$) because of the larger weak phase. It is similar to the case with the S-wave resonance K_0^* replaced by the P-wave resonance $K^*(892)$ in these decays [50]. But the sine values of the strong phases for these two kinds of decays have opposite signs. That is to say, $\sin \delta$ for the considered decays with the S-wave resonance K_0^* involved is positive, while that for the decays with the P-wave resonance $K^*(892)$ involved is negative.

The direct CP violation is just a number in the two-body framework, where the resonance mass is fixed during the calculations. While the CP violation under the three-body framework is dependent on the $K\pi$ invariant mass ω . We plot the differential distributions of the direct CP violations for the considered decays in Figures 2 and 3. In Figure 2, we can find that the differential distributions of the A_{CP} for the decay $B_c^+ \rightarrow \bar{K}_0^{*0}(1430) D_s^+ \rightarrow K^- \pi^+ D_s^+$ in both the BRW and LASS parametrizations are negative, those for the decay $B_c^+ \rightarrow K_0^{*0}(1430) D^+ \rightarrow K^+ \pi^- D^+$ are close to zero in the whole $K\pi$ invariant mass region. The differential distribution of the A_{CP} for the decay $B_c^+ \rightarrow K_0^{*+}(1430) D^0 \rightarrow K^0 \pi^+ D^0$ undergoes a sign flip in the BRW parametrization, while it is positive in the LASS form. In Figure 3, one can find that the differential distributions of the A_{CP} for the decays involving the $K_0^*(1950)$ in both the BRW and the LASS parametrizations are similar with each other, which might also indicate that the effect from nonresonant component in the $K_0^*(1950)$ is not as serious as that in the $K_0^*(1430)$.

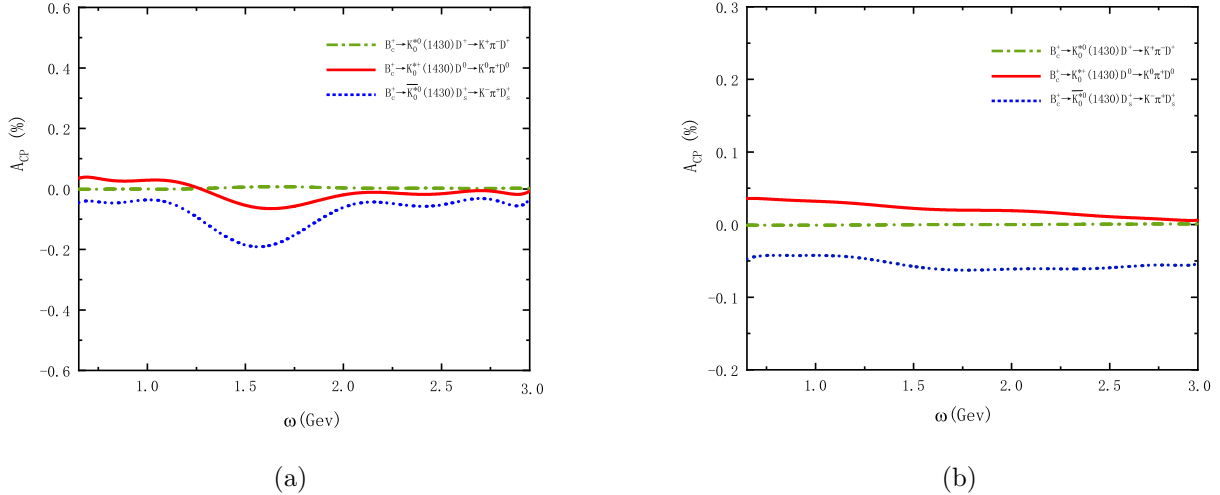


Figure 2: The differential distributions of A_{CP} in ω for the decays $B_c \rightarrow K_0^*(1430) D_{(s)} \rightarrow K\pi D_{(s)}$ obtained in the BRW (left) and the LASS (right) parametrizations.

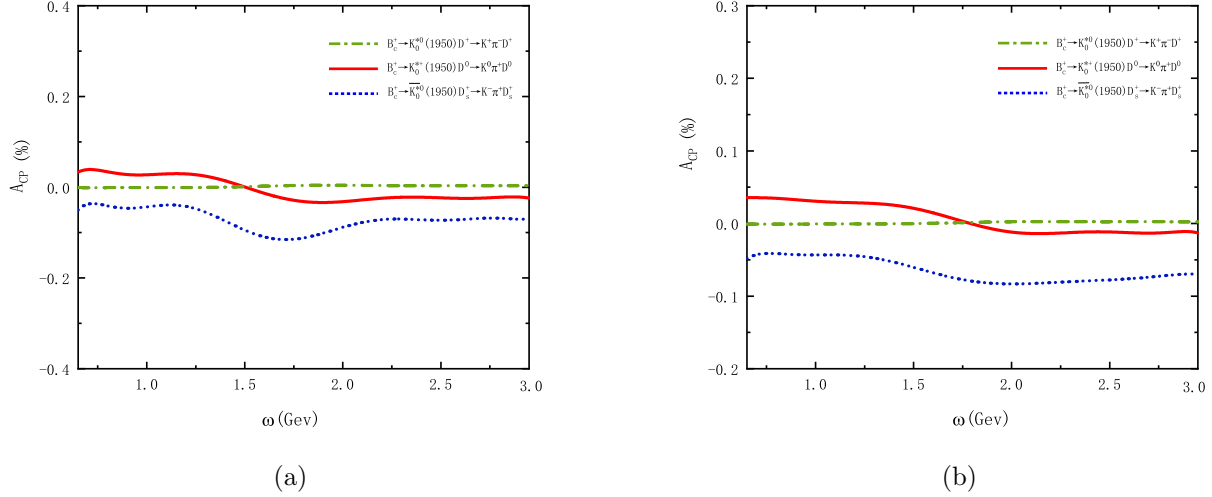


Figure 3: The differential distributions of A_{CP} in ω for the decays $B_c \rightarrow K_0^*(1950)D_{(s)} \rightarrow K\pi D_{(s)}$ obtained in the BRW (left) and the LASS (right) parametrizations.

IV. SUMMARY

In this paper, we studied the quasi-two-body decays $B_c \rightarrow K_0^*(1430, 1950)D_{(s)} \rightarrow K\pi D_{(s)}$ using the PQCD approach. The S-wave $K\pi$ pair DAs were introduced to describe the final-state interactions between K and π in the resonant region. As the crucial nonperturbative input, the time-like form factor $F_{K\pi}$ was parameterized by using two kinds of parametrizations, i.e., the LASS line shape and RBW model. Under the narrow width approximation and the isospin conservation, the branching ratios of these quasi-two-body decays can be related with those of the corresponding two-body decays $B_c \rightarrow K_0^*(1430, 1950)D_{(s)}$. We found that taking the LASS parametrization, both the branching ratios and the direct CP violations for the decays $B_c \rightarrow K_0^*(1430)D_{(s)}$ can be consistent with the previous PQCD calculations under the two-body framework by assuming $K_0^*(1430)$ as the lowest lying $q\bar{s}$ state (SII). Under the LASS parametrization, a slowly varying non-resonant component which interferes strongly with the resonance gives the dominant contribution to the large branching ratios with $10^{-5} \sim 10^{-4}$ order. As to the decays with $K_0^*(1950)$ involved, besides the two kinds of parametrizations, two decay width values $\Gamma_{K_0^*(1950)} = 0.201$ GeV and $\Gamma_{K_0^*(1950)} = 0.100$ GeV were used in the calculations. When taking $\Gamma_{K_0^*(1950)} = 0.201$ GeV, one can find that the branching ratios for the decays $B_c \rightarrow K_0^*(1950)D_{(s)}$ between these two parametrization schemes are close to each other, which are about one order smaller than those of the corresponding decays $B_c \rightarrow K_0^*(1430)D_{(s)}$. The effect from the non-resonant contribution in the decays with $K_0^*(1950)$ involved is not as serious as that in the channels with $K_0^*(1430)$ involved. These results can be tested by the future experiments.

Acknowledgment

This work is partly supported by the National Natural Science Foundation of China under Grant No. 11347030, by the Program of Science and Technology Innovation Talents in Universities of Henan Province 14HASTIT037, Natural Science Foundation of Henan Province under Grant No. 232300420116.

V. Appendix A: Some relevant functions

We show the explicit expressions of the hard functions h_i with $i = (a, \dots, h)$, which are obtained from the Fourier transform of the hard kernels

$$\begin{aligned}
h_i(\alpha, \beta, b_1, b_2) &= h_1(\beta, b_2) \times h_2(\alpha, b_1, b_2), \\
h_1(\beta, b_2) &= \begin{cases} K_0(\sqrt{\beta}b_2), & \beta > 0, \\ K_0(i\sqrt{-\beta}b_2), & \beta < 0, \end{cases} \\
h_2(\alpha, b_1, b_2) &= \begin{cases} \theta(b_2 - b_1) I_0(\sqrt{\alpha}b_1) K_0(\sqrt{\alpha}b_2) + (b_1 \leftrightarrow b_2), & \alpha > 0, \\ \theta(b_2 - b_1) I_0(\sqrt{-\alpha}b_1) K_0(i\sqrt{-\alpha}b_2) + (b_1 \leftrightarrow b_2), & \alpha < 0. \end{cases}
\end{aligned} \tag{45}$$

The jet function $S_t(x)$ resums the threshold logarithm $\ln^2 x$ appearing the hard kernels to all orders and is parameterized as

$$S_t(x) = \frac{2^{1+2a}\Gamma(3/2+a)}{\sqrt{\pi}\Gamma(1+a)} [x(1-x)]^a, \tag{46}$$

with the parameter $a = 0.4$.

The Sudakov factors used in the text are defined by

$$\begin{aligned}
S_{ab}(t) &= s\left(\frac{M_{B_c}}{\sqrt{2}}r_c, b_1\right) + s\left(\frac{M_{B_c}}{\sqrt{2}}x_3, b_3\right) + \frac{5}{3} \int_{1/b_1}^t \frac{d\mu}{\mu} \gamma_q(\mu) + 2 \int_{1/b_3}^t \frac{d\mu}{\mu} \gamma_q(\mu), \\
S_{cd}(t) &= s\left(\frac{M_{B_c}}{\sqrt{2}}r_c, b_1\right) + s\left(\frac{M_{B_c}}{\sqrt{2}}z, b\right) + s\left(\frac{M_{B_c}}{\sqrt{2}}(1-z), b\right) + s\left(\frac{M_{B_c}}{\sqrt{2}}x_3, b_1\right) \\
&\quad + \frac{11}{3} \int_{1/b_1}^t \frac{d\mu}{\mu} \gamma_q(\mu) + 2 \int_{1/b}^t \frac{d\mu}{\mu} \gamma_q(\mu), \\
S_{ef}(t) &= s\left(\frac{M_{B_c}}{\sqrt{2}}r_c, b_1\right) + s\left(\frac{M_{B_c}}{\sqrt{2}}z, b_3\right) + s\left(\frac{M_{B_c}}{\sqrt{2}}(1-z), b_3\right) + s\left(\frac{M_B}{\sqrt{2}}x_3, b_3\right), \\
&\quad + \frac{5}{3} \int_{1/b_1}^t \frac{d\mu}{\mu} \gamma_q(\mu) + 4 \int_{1/b_3}^t \frac{d\mu}{\mu} \gamma_q(\mu), \\
S_{gh}(t) &= s\left(\frac{M_{B_c}}{\sqrt{2}}z, b\right) + s\left(\frac{M_{B_c}}{\sqrt{2}}(1-z), b\right) + s\left(\frac{M_{B_c}}{\sqrt{2}}x_3, b_3\right) \\
&\quad + 2 \int_{1/b}^t \frac{d\mu}{\mu} \gamma_q(\mu) + 2 \int_{1/b_3}^t \frac{d\mu}{\mu} \gamma_q(\mu),
\end{aligned} \tag{47}$$

where K_0 and I_0 are modified Bessel functions with $K_0(ix) = \frac{\pi}{2}(-N_0(x) + iJ_0(x))$ and J_0 is the Bessel function. The hard scale t_i is chosen as the maximum of the virtuality of the internal momentum transition in the hard amplitudes

$$\begin{aligned}
t_a &= \max\left\{M_{B_c}\sqrt{|\alpha_a|}, M_{B_c}\sqrt{|\beta_a|}, 1/b_3, 1/b_1\right\}, & t_b &= \max\left\{M_{B_c}\sqrt{|\alpha_b|}, M_{B_c}\sqrt{|\beta_b|}, 1/b_1, 1/b_3\right\}, \\
t_c &= \max\left\{M_{B_c}\sqrt{|\alpha_c|}, M_{B_c}\sqrt{|\beta_c|}, 1/b_1, 1/b\right\}, & t_d &= \max\left\{M_{B_c}\sqrt{|\alpha_d|}, M_{B_c}\sqrt{|\beta_d|}, 1/b_1, 1/b\right\}, \\
t_e &= \max\left\{M_{B_c}\sqrt{|\alpha_e|}, M_{B_c}\sqrt{|\beta_e|}, 1/b_3, 1/b\right\}, & t_f &= \max\left\{M_{B_c}\sqrt{|\alpha_f|}, M_{B_c}\sqrt{|\beta_f|}, 1/b, 1/b_3\right\}, \\
t_g &= \max\left\{M_{B_c}\sqrt{|\alpha_g|}, M_{B_c}\sqrt{|\beta_g|}, 1/b, 1/b_1\right\}, & t_h &= \max\left\{M_{B_c}\sqrt{|\alpha_h|}, M_{B_c}\sqrt{|\beta_h|}, 1/b, 1/b_1\right\},
\end{aligned} \tag{48}$$

where

$$\begin{aligned}
\alpha_a &= r_b^2 - (\zeta + x_3(1 - \zeta))(1 - r^2), & \beta_a &= ((1 - x_3)(1 - \zeta) - r_c)(r_c - r^2), \\
\alpha_b &= (1 - \zeta - r_c)(r^2 - r_c), & \beta_b &= \beta_a \\
\alpha_c &= \beta_a, & \beta_c &= -((1 - \zeta)(1 - x_3) + \zeta - r_c)((1 - r^2)(1 - z) + r^2 - r_c), \\
\alpha_d &= \beta_a, & \beta_d &= -((1 - \zeta)(1 - x_3) - r_c)((1 - r^2)z + r^2 - r_c); \\
\alpha_e &= -zx_3(1 - \zeta)(1 - r^2), & \beta_e &= r_b^2 - (1 - x_3(1 - \zeta) - r_c)(1 - x_2(1 - r^2) - r_c), \\
\alpha_f &= \alpha_e, & \beta_f &= r_c^2 - (r_c - x_3(1 - \zeta))(r_c - z(1 - r^2)). \\
\alpha_g &= -(\zeta + x_3(1 - \zeta))(1 - r^2), & \beta_g &= \alpha_e, \\
\alpha_h &= r_c^2 - (1 - \zeta)(z(1 - r^2) + r^2), & \beta_h &= \alpha_e.
\end{aligned} \tag{49}$$

References

- [1] R. Aaij *et al.* (LHCb Collaboration), Phys. Rev. D **92**, 012012 (2015) [arXiv:1505.01505 [hep-ex]].
- [2] R. Aaij *et al.* (LHCb Collaboration), Phys. Rev. D **105**, 072005 (2022) [arXiv:2112.11428 [hep-ex]].
- [3] R. Aaij *et al.* (LHCb Collaboration), Phys. Rev. D **90**, 072003 (2014) [arXiv:1407.7712 [hep-ex]].
- [4] R. Aaij *et al.* (LHCb Collaboration), Phys. Rev. D **98**, 072006 (2018) [arXiv:1807.01891 [hep-ex]].
- [5] R. Aaij *et al.* (LHCb Collaboration), Phys. Rev. D **94**, 072001 (2016) [arXiv:1608.01289 [hep-ex]].
- [6] B. Meadows, eConf C070805 (2007) 27 [arXiv:0712.1605 [hep-ex]].
- [7] D. Aston *et al.* (LASS collaboration), Nucl. Phys. B **296**, 493 (1988).
- [8] A. Garmash *et al.* (Belle collaboration), Phys. Rev. Lett. **96**, 251803 (2006) [arXiv:hep-ex/0512066].
- [9] B. Aubert *et al.* (BaBar collaboration), Phys. Rev. D **78**, 012004 (2008) [arXiv:0803.4451 [hep-ex]].
- [10] W. F. Wang, J. Chai and A. J. Ma, JHEP **03**, 162 (2020) [arXiv:2001.00355 [hep-ph]].
- [11] W. S. Fang, Z. T. Zou and Y. Li, Phys. Rev. D **108**, 113007 (2023) [arXiv:2311.17678 [hep-ph]].
- [12] J. P. Lees *et al.* (BaBar Collaboration), Phys. Rev. D **104**, 072002 (2021) [arXiv:2106.05157 [hep-ex]].
- [13] I. P. Gouzev, V. V. Kiselev, A. K. Likhoded, V. I. Romanovsky and O. P. Yushchenko, Phys. Atom. Nucl. **67**, 1559 (2004) [arXiv:hep-ph/0211432].
- [14] R. Aaij *et al.* (LHCb Collaboration), Phys. Rev. D **94**, 091102 (2016) [arXiv:1607.06134 [hep-ex]].
- [15] R. Aaij *et al.* (LHCb Collaboration), Phys. Rev. D **95**, 032005 (2017) [arXiv:1612.07421 [hep-ex]].
- [16] Z. T. Zou, Y. Li and X. Liu, Phys. Rev. D **97**, 053005 (2018) [arXiv:1712.02239 [hep-ph]].
- [17] B. Bhattacharya, M. Gronau and J. L. Rosner, Phys. Lett. B **726**, 337 (2013) [arXiv:1306.2625 [hep-ph]].
- [18] M. Gronau, Phys. Lett. B **727**, 136 (2013) [arXiv:1308.3448 [hep-ph]].
- [19] D. Xu, G. N. Li and X. G. He, Phys. Lett. B **728**, 579 (2014) [arXiv:1311.3714 [hep-ph]].
- [20] M. Gronau and J. L. Rosner, Phys. Rev. D **72**, 094031 (2005) [arXiv:hep-ph/0509155].
- [21] G. Engelhard and G. Raz, Phys. Rev. D **72**, 114017 (2005) [arXiv:hep-ph/0508046].
- [22] M. Imbeault and D. London, Phys. Rev. D **84**, 056002 (2011) [arXiv:1106.2511 [hep-ph]].
- [23] X. G. He, G. N. Li and D. Xu, Phys. Rev. D **91**, 014029 (2015) [arXiv:1410.0476 [hep-ph]].
- [24] S. H. Zhou, R. H. Li, Z. Y. Wei and C. D. Lu, Phys. Rev. D **104**, 116012 (2021) [arXiv:2107.11079 [hep-ph]].

- [25] S. Kränkl, T. Mannel and J. Virto, Nucl. Phys. B **899**, 247 (2015) [arXiv:1505.04111 [hep-ph]].
- [26] H. Y. Cheng, C. K. Chua and Z. Q. Zhang, Phys. Rev. D **94**, 094015 (2016) [arXiv:1607.08313 [hep-ph]].
- [27] Y. Li, Phys. Rev. D **89**, 094007 (2014) [arXiv:1402.6052 [hep-ph]].
- [28] H. Y. Cheng, C. K. Chua and A. Soni, Phys. Rev. D **76**, 094006 (2007) [arXiv:0704.1049 [hep-ph]].
- [29] R. Klein, T. Mannel, J. Virto and K. K. Vos, JHEP **10**, 117 (2017) [arXiv:1708.02047 [hep-ph]].
- [30] Y. C. Zhao, Z. Q. Zhang, Z. Y. Zhang, Z. J. Sun and Q. B. Meng, Chin. Phys. C **47**, 073104 (2023) [arXiv:2304.13286 [hep-ph]].
- [31] Z. Q. Zhang, Y. C. Zhao, Z. L. Guan, Z. J. Sun, Z. Y. Zhang and K. Y. He, Chin. Phys. C **46**, 123105 (2022) [arXiv:2207.02043 [hep-ph]].
- [32] Z. Q. Zhang and H. X. Guo, Eur. Phys. J. C **79**, 59 (2019) [arXiv:1812.11372 [hep-ph]].
- [33] Y. Li, W. F. Wang, A. J. Ma and Z. J. Xiao, Eur. Phys. J. C **79**, 37 (2019) [arXiv:1809.09816 [hep-ph]].
- [34] A. J. Ma, Y. Li, W. F. Wang and Z. J. Xiao, Phys. Rev. D **96**, 093011 (2017) [arXiv:1708.01889 [hep-ph]].
- [35] C. H. Chen and H. n. Li, Phys. Rev. D **70**, 054006 (2004) [arXiv:hep-ph/0404097].
- [36] C. H. Chen and H. n. Li, Phys. Lett. B **561**, 258 (2003) [arXiv:hep-ph/0209043].
- [37] T. Kurimoto, H. n. Li and A. I. Sanda, Phys. Rev. D **67**, 054028 (2003) [arXiv:hep-ph/0210289].
- [38] R. H. Li, C. D. Lu and Z. Hao, Phys. Rev. D **78**, 014018 (2008) [arXiv:0803.1073 [hep-ph]].
- [39] H. Y. Cheng, C. K. Chua, K. C. Yang and Z. Q. Zhang, Phys. Rev. D **87**, 114001 (2013) [arXiv:1303.4403 [hep-ph]].
- [40] H. Y. Cheng, C. K. Chua and K. C. Yang, Phys. Rev. D **73**, 014017 (2006) [arXiv:hep-ph/0508104].
- [41] M. Jamin, J. A. Oller and A. Pich, Nucl. Phys. B **622**, 279 (2002) [arXiv:hep-ph/0110193].
- [42] D. R. Boito and R. Escribano, Phys. Rev. D **80**, 054007 (2009) [arXiv:0907.0189 [hep-ph]].
- [43] U. G. Meißner and W. Wang, Phys. Lett. B **730**, 336-341 (2014) [arXiv:1312.3087 [hep-ph]].
- [44] K. Maltman, Phys. Lett. B **462**, 14 (1999) [arXiv:hep-ph/9906267].
- [45] C. M. Shakin and H. Wang, Phys. Rev. D **63**, 074017 (2001).
- [46] H. Y. Cheng and C. K. Chua, Phys. Rev. D **88**, 114014 (2013) [arXiv:1308.5139 [hep-ph]].
- [47] B. Aubert *et al.* (BaBar Collaboration), Phys. Rev. D **72**, 072003 (2005) [arXiv:hep-ex/0507004].
- [48] G. Buchalla, A. J. Buras and M. E. Lautenbacher, Rev. Mod. Phys. **68**, 1125 (1996) [arXiv:hep-ph/9512380].
- [49] R. L. Workman *et al.* [Particle Data Group], Review of Particle Physics, PTEP **2022**, 083C01 (2022).
- [50] Z. Y. Zhang, Z. Q. Zhang, S. Y. Wang, Z. J. Sun and Y. Y. Yang, Phys. Rev. D **108**, 076009 (2023) [arXiv:2307.12351 [hep-ph]].
- [51] B. Aubert *et al.* (BaBar Collaboration), Phys. Rev. Lett. **99**, 161802 (2007) [arXiv:0706.3885 [hep-ex]].
- [52] H. Y. Cheng, C. W. Chiang and C. K. Chua, Phys. Rev. D **103**, 036017 (2021) [arXiv:2011.07468 [hep-ph]].
- [53] Y. L. Shen, W. Wang, J. Zhu and C. D. Lu, Eur. Phys. J. C **50**, 877 (2007) [arXiv:hep-ph/0610380].